Research Article

T. S. Sachit, Arunkumar Bongale*, Satish Kumar, and Priya Jadhav

Wear performance analysis of B_4C and graphene particles reinforced Al–Cu alloy based composites using Taguchi method

https://doi.org/10.1515/jmbm-2022-0274
received June 10, 2022; accepted November 29, 2022

Abstract: In this study, the wear performance of boron carbide (B_4C) and graphene (Gr) particles reinforced Al–Cu alloy composites was investigated. The composite samples were made using the solid-state manufacturing process. The wear performance was assessed using a pin-on-disc tribometer. The Taguchi optimization approach was used to determine the performance of each parameter. All experiments were carried out using the L27 array, which included three sets of parameters such as applied load, disc speed, and reinforcement percentage. The ANOVA approach was used to examine the impact of each parameter. According to the findings, the weight on the pin has the greatest influence on wear, followed by sliding speed and reinforcing percentage. The addition of B_4C particles improves the wear resistance, and the Gr functions as a self-lubricating agent while in use. Scanning electron microscope analysis of worn-out samples revealed an abrasive type of wear process.

Keywords: dry sliding wear, metal matrix composite, boron carbide particles, graphene particles, Taguchi method

1 Introduction

Metal matrix composites (MMCs) are the new grade of composite materials reinforced with advanced hard ceramic particles. Generally, the properties of this class of composites were enhanced by different types of reinforcement particles. The properties like good strength, good wear resistance, high thermal strength, and good corrosion resistance can be enhanced by using different combinations of reinforcements [1]. MMCs reinforced with ceramic particles have high demand in automotive industries, space applications, defense field, electronic parts manufacturing, and so on [2]. The selection of matrix and reinforcement materials is purely based on the area of application and the property of the developed composite that depends on the method of manufacturing. In General, aluminum is highly used matrix material due to its lightweight and less cost. The different classes of aluminum are used for some specific applications. Apart from this, some special type of alloys like magnesium (Mg), copper (Cu), and titanium (Ti) are used for some specific property requirements. The hard reinforcement particles show acceptable remarks on the property enhancement in composites. Silicon carbide (SiC) and boron carbide (B_4C) are commonly used hard ceramic particles because of low density and good wettability. TiC, TiO_2, and Al_2O_3 are some of the particles which are used in specific requirements. The alloy Al–Cu combination matrix possess high strength during normal working conditions over other classes of Al alloys and thus gain the focus to perform as an excellent matrix material for the composites [3]. The uniform dispersion of the particles can be achieved in Al–Cu series alloys and they form a barrier to the movement of the dislocation in the overheat treatment. Therefore, Al–Cu alloy was preferred as a matrix material in this work and stir casting was the selected process. The reinforcement particles also increase the bonding strength thereby supporting in carrying the applied load so that they can help in preventing the quick failure. B_4C is one of the hard ceramic particles with less density and high stiffness

* **Corresponding author: Arunkumar Bongale,** Department of Robotics and Automation, Symbiosis Institute of Technology (SIT), Symbiosis International (Deemed University), Lavale, Pune-412 115, Maharashtra State, India, e-mail: arunbongale1980@gmail.com
T. S. Sachit, Priya Jadhav: Department of Robotics and Automation, Symbiosis Institute of Technology (SIT), Symbiosis International (Deemed University), Lavale, Pune-412 115, Maharashtra State, India
Satish Kumar: Department of Robotics and Automation, Symbiosis Institute of Technology (SIT), Symbiosis International (Deemed University), Lavale, Pune-412 115, Maharashtra State, India; Symbiosis Centre for Applied Artificial Intelligence, Symbiosis International (Deemed University), Lavale, Pune-412 115, Maharashtra State, India

and good hardness property. Hence, Al–B_4C composites possess improved hardness and good stiffness [4]. However, the high brittleness of the B_4C particles leads to the inherent drawback in its use as a reinforcement in some applications. However, to overcome this drawback and to enhance the mechanical properties of the ceramics, filler materials can be used. Carbon nanotubes and graphene (Gr) powders are used as a protective material in composites. Gr is a lightweight material having 2.2 g/cc of density. Gr is having similar structure as carbon atoms, but it is flat or cylindrical in shape. Gr exhibits good mechanical and thermal properties due to its unique structure.

Many research works were carried out on Al-reinforced ceramics to understand the mechanical and wear resistance properties. Composites can be developed using different processing techniques by changing the percentage of reinforcements. Manivannan *et al.* [5] studied the Al6061–SiC–Gr hybrid nano composites. Addition of nano scale SiC and Gr particles improves the surface roughness and showed good wear resistance properties by addition of self-lubricating filler. Harichandran *et al.* [6] worked on the mechanical properties of the Al-reinforced with nano and micro B_4C particles using ultrasonic cavitation method. Nano particles show better results than micro particles. Also, the wear resistance increased with the increase in particle percentage up to 8%. Qiu *et al.* [7] studied the SiC nano particles reinforced with Al–Cu particles using semisolid stirring and ball milling method. The particles distribution was analyzed using X-ray powder diffraction (XRD) and Scanning electron microscope (SEM). The nano particles were strongly reinforced. The mechanical properties of the composites are improved by adding nano SiC particles. The major improvement in tensile strength of the composite was due to the incorporation of SiC particles and good interfacial bonding between SiC and Al–Cu alloy. Pan *et al.* [8] prepared a high-performance copper-based composite using powder metallurgy by different techniques such as acid-mix treatment, molecular method, ball milling, and plasma sintering, and investigated their mechanical properties, microstructure, electrical conductivity, *etc.* It was concluded that adding aluminum oxide nanoparticles (NPs) to it worked as an effective mixing agent to distribute CNT in Cu powder and enhance adhesion between them improving the tensile strength, hardness, yield strength, elongation, *etc.* Similarly, Koga *et al.* [9] gave a different perspective for the application of quasi-crystalline composites forming a microstructure enclosing the quasi-crystalline, Al_7Cu_2Fe and Al phase by casting an alloy that was arc-melted, annealed, and characterized by XRD, SEM, TEM, *etc.* In a recent research, Kim *et al.* [10] fabricated the Al–Cu composites using spark plasma sintering and studied the effects of adding copper varying the weight percentage on physical and thermal properties. The findings reveal that the addition of copper improves the performance of the composites. Another research by Güler and Bağcı [11] included the investigation of effects of aluminum oxide addition and silver coating on the physical properties of copper matrix-based composites fabricated by electroless plating and hot pressing. Kumar *et al.* [12] adopted powder metallurgy for fabricating the composites and characterized the effects of normalizing and quenching medium *i.e.*, water and oil on wear and friction of self- lubricating Al–Cu matrix composites. The powder metallurgy method makes sure that there is proper distribution of the reinforcement particles and proper bonding between the matrix and reinforcements. Mei *et al.* [13] investigated the mechanical properties of copper ions added to graphene oxide–Al powder to improve its distribution on aluminum by a simple electrostatic adsorption method. The addition of copper ions can improve the performance of the composite. Bhoi *et al.* [14] used copper–tin alloy reinforced by SiC particles and aluminum oxide as an abrasive material by varying its percentage of graphite powder as a friction modifier. The developed new brake material was tested using pin on disc machine to check its wear and friction. Results indicate that there is an improvement in wear resistance by the addition of SiC particles and aluminum oxide rubs over the disc material and minimizes the material removal rate. Castañeda-Vía *et al.* [15] developed an aluminum–iron–copper based composite and investigated their mechanical properties. XRD and SEM analysis were done using Fourier transform Raman spectroscopy. These experimental results indicate the addition of Gr to improve the wear resistance and help in lubrication. It is understood that the increase in the weight percentage of mono B_4C particles by adding small amount of Gr powder can drastically improve the tribological properties of the developed composites. Also, the effect of particles size of the B_4C can drastically improve the performance of the composites and the larger particle size reduces the problem of agglomeration and results in more homogeneous particle distribution. A recent work by Weng *et al.* [16] includes synthetization of copper NPs and their attachment to the surface of Al powder particles with the help of a polydopamine (PDA) coating which showed improved sintering behavior. The varying sintering temperature can affect the performance of the composites. The less sintering temperature can reduce the bonding between matrix and reinforcement and high sintering temperature can lead to the reduced solidification and thereby reduces the strength of the composites.

Based on the research studies, how the MMCs show their significant performance by enhancing the properties in different applications, current work focuses on development and experimentation of Al–Cu matrix reinforced with B_4C and Gr particles with varying percentage of reinforcement using powder compaction method.

2 Materials and method

In the present research work, Al–Cu powders are used as a matrix material. Al with 6wt% copper weight percentage was maintained in the matrix mixture. B_4C particles with varying percentage of reinforcement was used as a reinforcement material and Gr particle is used as binder material [17]. The composites are fabricated using solid state fabrication method. The powder compaction method is one of the techniques which is used to fabricate the composites. As compared with other fabrication methods, the powder compaction method has significant effect in gaining the fine grain structures and maintains the chemically homogeneousness of the powders. The properties of the powder compacted composites enhance owing to the proper distribution of the nano B_4C particles with Al–Cu alloy powders [1]. The powder compaction method has significant effect in gaining the fine grain structures and maintains the chemical homogeneity of powders. The properties of the powder compacted composites enhance owing to the proper distribution of the nano B_4C particles in the Al–Cu alloy powders [1]. The die which is used to compact the powder has a cylinder and top and bottom plungers. Hydraulic pressing machine of capacity 5 ton is used to compact the powder particles. The weighed amount of Al–Cu powder and B_4C particles are mixed well using a planetary ball mill and poured into the die. To avoid material contamination on the inner wall of the cylinder, zinc stearate solution is applied on the walls of plunger and cylinder [18]. Figure 1 shows the powder compaction method. The PVA is added to the mixtures to enable proper bonding between the Al–Cu and B_4C.

The percentage of reinforcement was maintained at 2, 4, and 6 wt% for B_4C particles and a constant 3 wt% of Gr was maintained for all the samples. Table 1 shows the % reinforcement B_4C and Gr used to develop the composite. After compaction of the samples, sintering was carried out under controlled environment to avoid further oxidation of the samples [19]. A vacuum chamber temperature was gradually increased up to 500°C for time duration of 90 min. The phases present in the powder particles were found using the XRD and the element

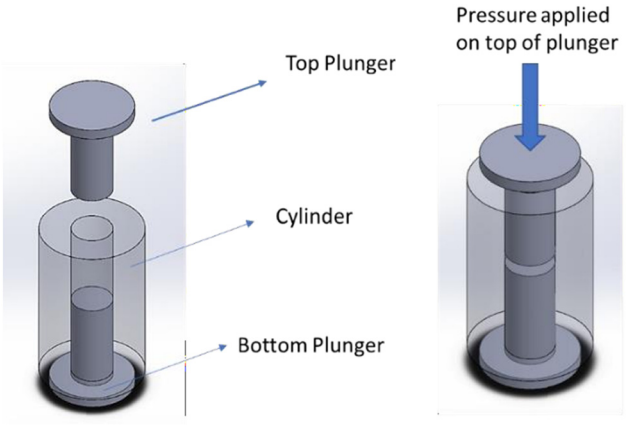

Figure 1: Powder compaction method.

confirmation was done by using EDS analysis. The average particle size was analyzed using SEM analysis.

Figure 2a–d shows the EDS analysis of the matrix and reinforcement powders. From Figure 2a, the spectra of Al were detected and there were no other elements present in the powder so that there were no other impurities present in the powder. Similar results can be seen in spectra of Cu.

Figure 2b depicts the EDS analysis and its elemental mapping of Cu can be seen. Figure 2c shows the elemental mapping for B_4C particles and it was observed that the boron and carbide phases were present in the powder. No other elements were observed in the powder. Figure 2d shows the elemental mapping for Gr powder. It was observed that 99 % of carbon element was present in the Gr and less than <1% of associated elements can be observed in the powder.

Figure 3a and b depicts the SEM images of the Al powder with different magnifications. It was observed from the SEM result that the uniform particle size was maintained throughout the volume. Figure 4a and b shows the SEM images of Cu powder with different magnifications. Figure 5a and b shows the SEM images of B_4C particles with different magnifications. Figure 6a and b shows the SEM images of Gr particles with different magnifications.

The XRD was recorded for all the compositions room temperature. Strong and intense peaks corresponding to

Table 1: Labeling of composite samples

Sample label	B_4C (wt%)	Gr (wt%)
A23	2	3
A43	4	3
A63	6	3

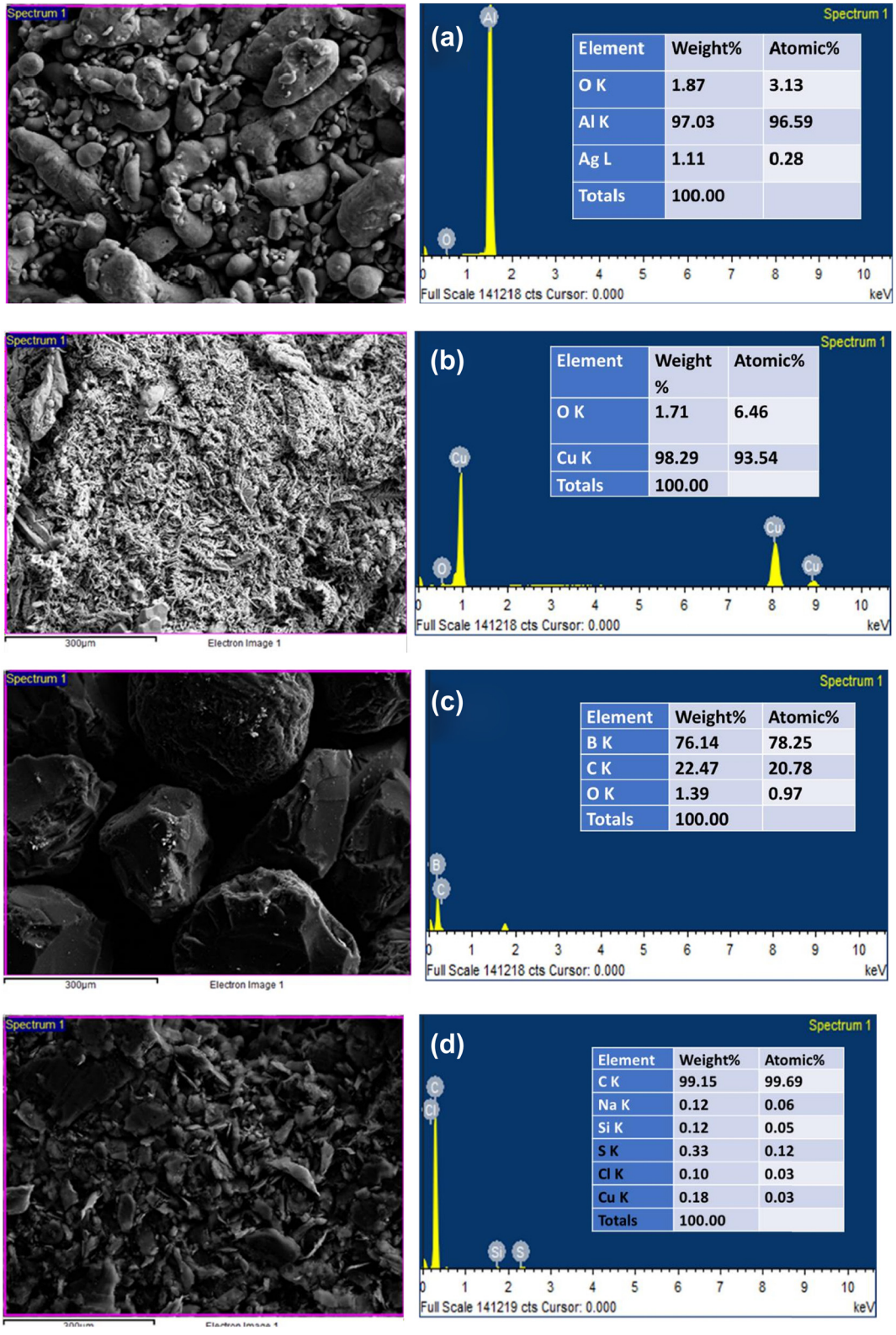

Figure 2: (a) EDS analysis of the Al powder and its SEM image. (b) EDS analysis of the Cu powder and its weight percentage. (c) EDS analysis of B_4C particles and its weight percentage. (d) EDS analysis of Gr powder and its phases.

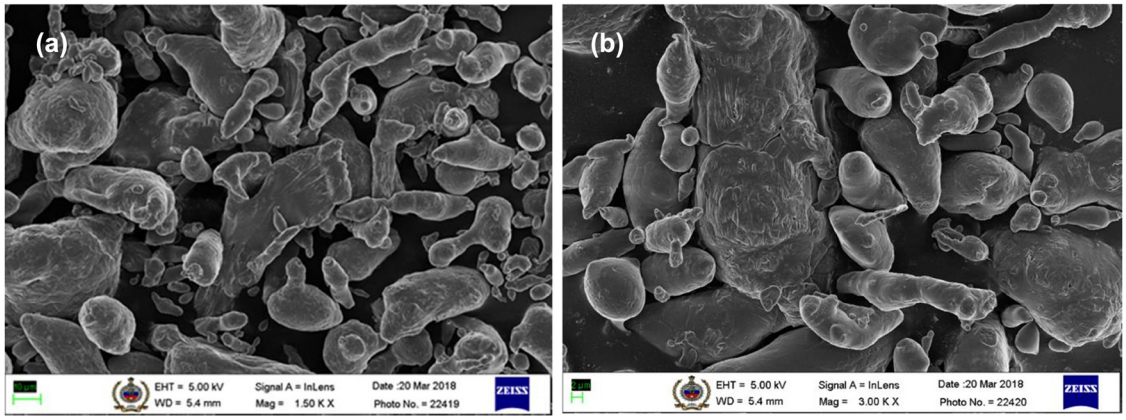

Figure 3: (a) and (b) SEM images of Al particles with different magnifications.

Al, Cu, and Gr were identified from the diffractogram, as shown in Figure 7. It was seen that the peaks resembled that of Al and Cu which formed the base matrix. The trace of B_4C was less than the detectable limit. The CIF files obtained from the materials studio for Al and Cu matched perfectly with the data obtained. Both Al and Cu was present in the cubic closed packing structure with a space group of "Fm3m". The average crystal size for all the compositions was calculated using the Debye Scherrer equation.

$$D = \frac{0.9\lambda}{\beta\cos\theta},$$

where, D, 0.9, λ, β, and θ are the crystallite size, size constant, wavelength, full width half maximum (FWHM), and the angle of diffraction, respectively. The average crystal size was calculated using all reflections across the 2θ range of 20–85°.

It was seen that there was a shift in the peaks corresponding to Al and Cu, which confirms the variation in lattice cell parameters. Such a change is a signature of distortion of the lattice cell parameters due to the incorporation of guest element into its structure. However, it was interesting to notice that, at high % of Gr, the intensity corresponding to Al and Cu reflections fell to almost half which is an indication of loss of crystallinity due to lattice cell distortion. Figure 8a and b shows the SEM images of the developed samples took under different magnifications. The SEM images confirm the presence of B_4C particles in the composites.

3 Experimental method

3.1 Hardness test

Hardness of the developed samples were assessed by using Vickers micro hardness test. The test specimens were polished using polishing machine with different grade sand papers and finally the mirror finished surface was obtained by polishing using diamond abrasive [20]. Hardness test was performed under ASTM E 384-10

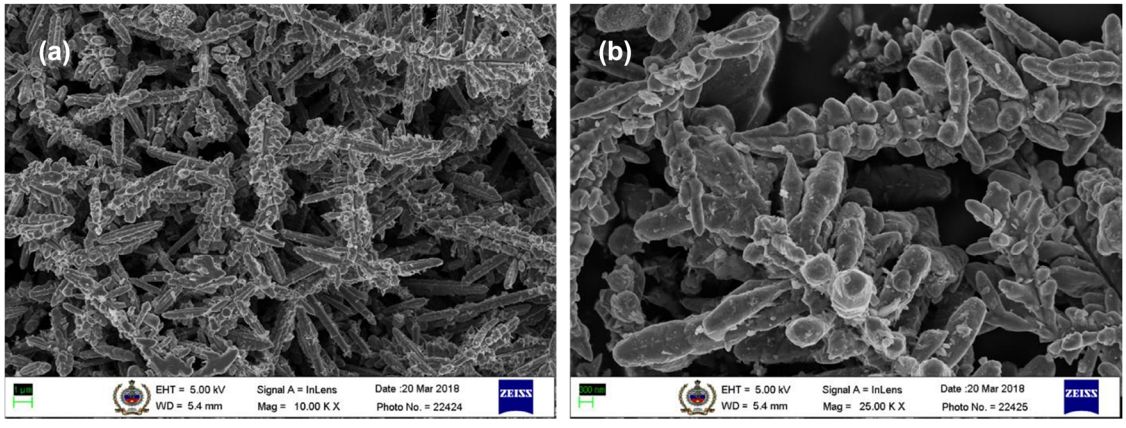

Figure 4: (a) and (b) SEM images of Cu powder at different magnifications.

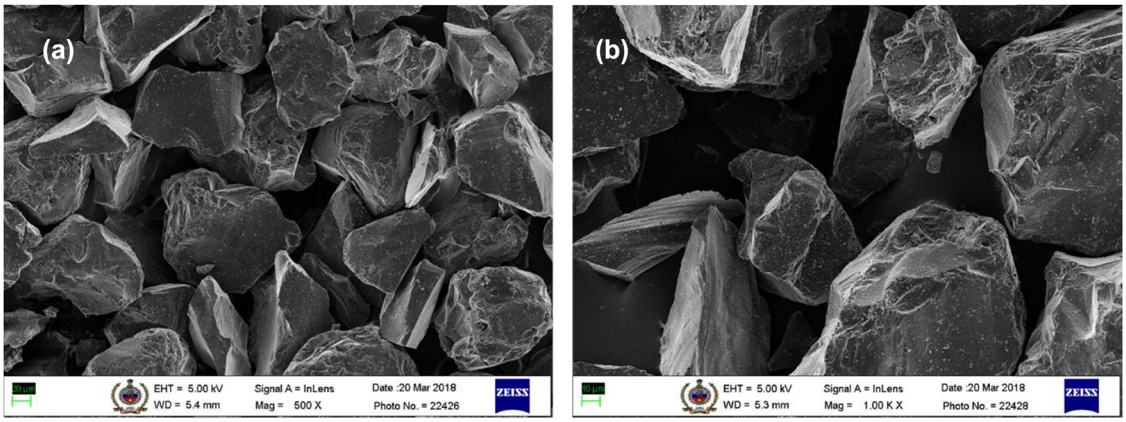

Figure 5: (a) and (b) SEM images of B_4C particles at different magnifications.

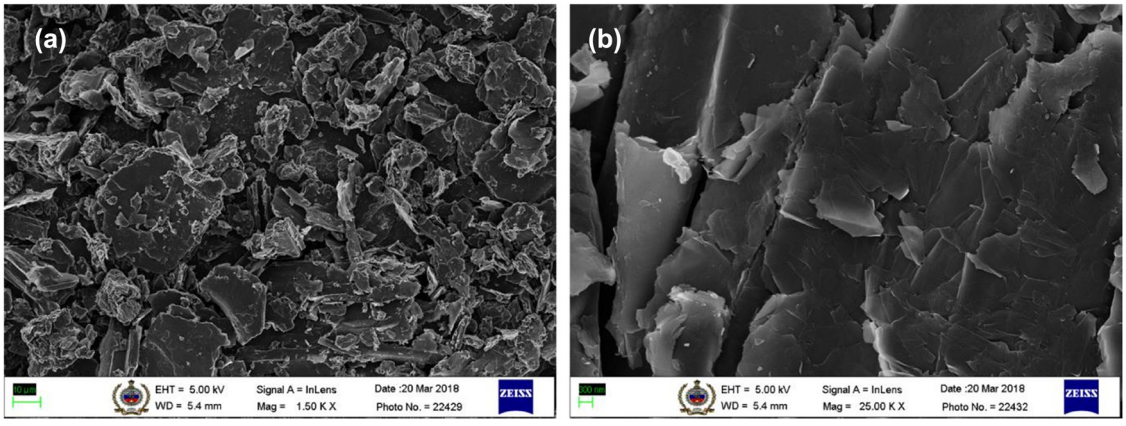

Figure 6: (a) and (b) SEM images of Gr powder at different magnifications.

standards [21]. Totally five indentations were made on the surface of the sample to avoid the impression of indention on the reinforcement particle. All the samples were tested with an average load of 300 g with a time duration of 10 s [22]. The average of the all the five readings were reported.

3.2 Dry sliding wear

Dry sliding wear tests were performed using pin-on-disc tribometer as per ASTM G99 standard [23]. All the samples were tested under room temperature and no lubricants were used during testing. The three different test parameters were chosen to identify the optimum wear rate among the developed composites. Table 2 shows the chosen test factors and levels.

The wear test was done by holding the pin stationary over the rotating disc. The steel disc En-35 with a surface roughness of less than 0.5 µm was used [24]. The rotating diameter of 100 mm was kept for all the experiments. The wear rate was calculated by taking the initial and final weight of the pin before and after the test. The wear rate

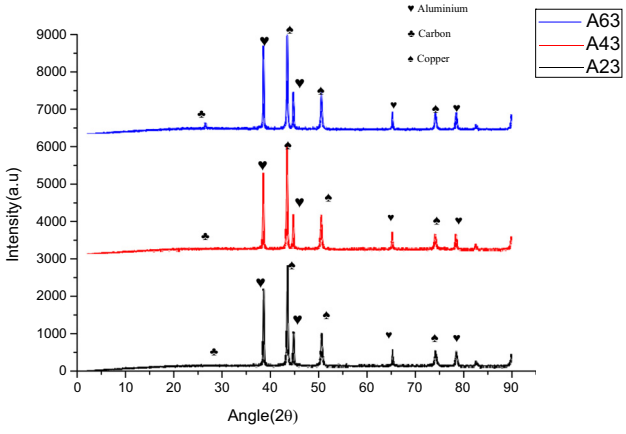

Figure 7: XRD data of pristine and composite materials recorded at room temperature.

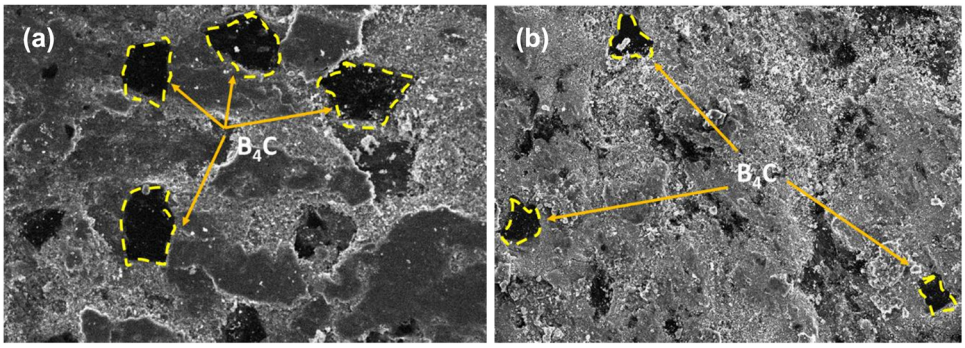

Figure 8: (a) and (b) SEM images of A43 and A63 samples under different magnifications.

was measured by means of weight loss per minute. All the tests were conducted for 10 min of time, so that the final wear rate value was measured in terms of g/min.

3.3 Taguchi optimization technique

Taguchi approach was incorporated to understand the effect of parameters and to identify the optimum wear value [25]. From the selected parameters and their levels in Table 2, A3 level 3 factor was designed using Minitab 16 software. L27 design was chosen to perform the experiments with the obtained orthogonal array. A total of 27 experiments were carried out with interactions between each parameter. The level of significance was identified by the signal to noise (S/N) ratio obtained from the results. The "smaller is the better" characteristic was chosen to detect the rank of the factor [26]. Table 4 depicts the L27 orthogonal array, and the wear rate values obtained.

4 Results and discussion

4.1 Microhardness

The results of microhardness test conducted on A23, A43, and A63 samples are shown in Table 3. The results reveled that the addition of hard B_4C particles increases the hardness of the composites. It was observed that the hardness values significantly improved with the addition of B_4C particles and the addition of Gr also showed some influence on the hardness value. Pure Al–Cu alloy sample was developed without adding B_4C and Gr. The results were compared long with reinforced samples.

4.2 Wear rate analysis

Wear rate analysis was carried out by conducting the experiments as per Taguchi design of experiments and the results are shown in Table 4.

The wear results show that the maximum wear rate was found under high applied load condition. When the load applied on the pin increases, the amount of metal removal rate increases. From the wear table, it was observed that the minimum wear rate was obtained at high load condition. The disc speed also shows some influence on wear rate, as the speed increases, the wear rate increases. But the B_4C reinforcement shows better resistance on wear rate. When B_4C percentage increases, the wear rate decreases. The maximum wear rate occurred for the specimen of 2wt% B_4C particles and disc speed of 400 rpm when the specimen load was 25 N. Similarly, the minimum wear rate was obtained at 6wt% B_4C, 200 rpm disc speed with 15 N of applied load.

Table 2: Wear test parameters and levels

Applied load (N)	Disc speed (rpm)	B_4C (wt%)	Gr (wt%)
15	200	2	3
20	300	4	3
25	400	6	3

Table 3: Microhardness results of with and without adding B_4C and Gr particles

Sample label	B_4C (wt%)	Gr (wt%)	Vickers Microhardness
A00	—	—	49
A23	2	3	63
A43	4	3	78
A63	6	3	90

Table 4: Taguchi L27 with wear and response data

S. No.	Load (N)	Speed (rpm)	B_4C (wt%)	Wear (g/min $\times 10^{-3}$)	S/N ratio
1	15	200	2	0.2674	11.456
2	15	200	4	0.2526	11.951
3	15	200	6	0.2189	13.195
4	15	300	2	0.2737	11.254
5	15	300	4	0.2674	11.456
6	15	300	6	0.2256	12.933
7	15	400	2	0.2918	10.698
8	15	400	4	0.2746	11.225
9	15	400	6	0.2623	11.624
10	20	200	2	0.3274	9.698
11	20	200	4	0.2837	10.942
12	20	200	6	0.2692	11.398
13	20	300	2	0.3592	8.893
14	20	300	4	0.3325	9.564
15	20	300	6	0.3083	10.220
16	20	400	2	0.3673	8.699
17	20	400	4	0.3416	9.329
18	20	400	6	0.3179	9.954
19	25	200	2	0.4385	7.160
20	25	200	4	0.4263	7.405
21	25	200	6	0.3896	8.187
22	25	300	2	0.4659	6.634
23	25	300	4	0.4025	7.904
24	25	300	6	0.3936	8.098
25	25	400	2	0.5262	5.576
26	25	400	4	0.5037	5.956
27	25	400	6	0.4772	6.425

4.3 S/N response and ANOVA

The response of individual parameter on the wear rate of the developed samples can be evaluated using S/N response table by means of rank. Table 5 shows the S/N ratio response of each parameter. The most inducing parameter on the wear rate was the applied load and that has been ranked as 1, followed by disc speed having nominal influence on wear rate that has been ranked as 2. Even the B_4C reinforcement percentage a shows some nominal influence on the wear rate and that has been ranked as 3. The main effect plot of means of applied load, disc speed, and weight percentage of B_4C are was shown in Figure 9. The smaller is the better model was chosen for the analysis. It was observed that the applied load of 15 N shows the minimum response on wear rate, similarly 200 rpm of disc speed and 6wt% of B_4C shows the minimum response on wear rate of the composites.

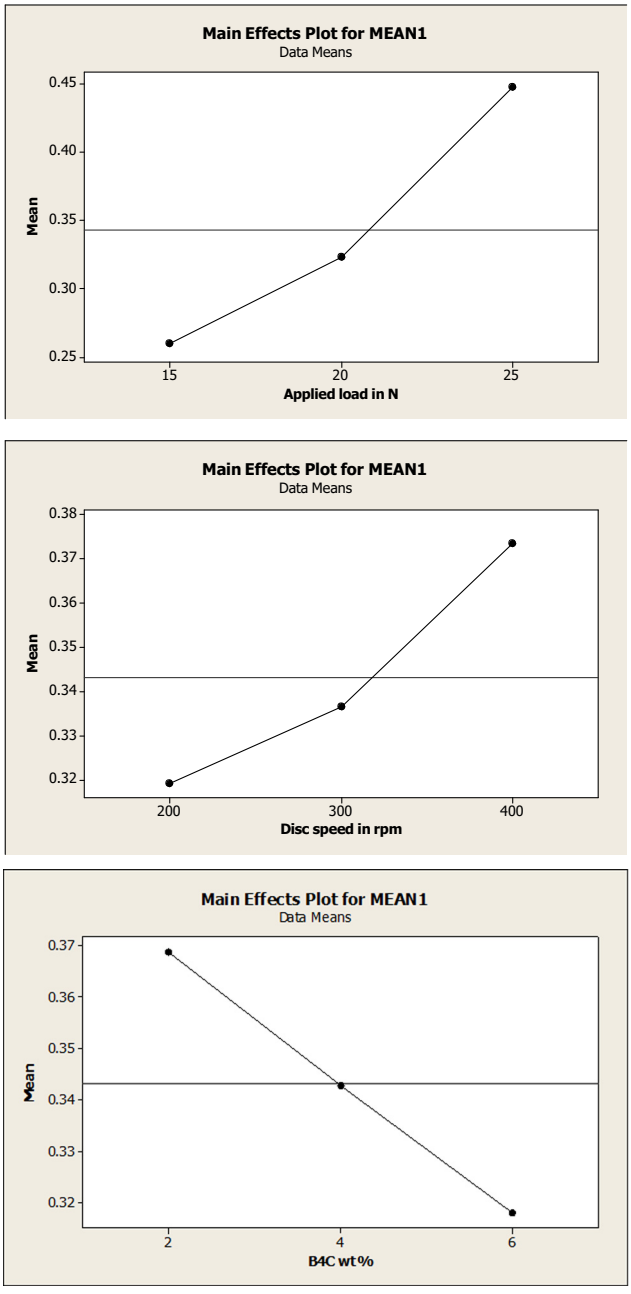

Figure 9: Main effect plot of means of applied load, disc speed, and B_4C wt%.

Table 5: S/N response table

Level	Applied load (N)	Disc speed (rpm)	B_4C (wt%)
1	0.2594	0.3193	0.3686
2	0.323	0.3365	0.3428
3	0.4471	0.3736	0.3181
Delta	0.1877	0.0543	0.0505
Rank	1	2	3

Table 6 reveals the ANOVA results obtained from the available wear rate data. The influence of each parameter on the wear rate was analyzed using ANOVA data.

Table 6: Wear rate analysis using ANOVA

Factors	DF	Seq SS	Adj SS	Adj MS	*F*	*P*	*P* (%)
Load in N	2	0.164	0.164	0.082	238.56	0	83.57
Speed in rpm	2	0.014	0.014	0.00694	20.19	0	7.072
B_4C wt%	2	0.011	0.011	0.00575	16.72	0	5.857
Error	20	0.007	0.007	0.00034			3.503
Total	26	0.196					

S = 0.0185398, R-Sq = 96.50%, R-Sq(adj) = 95.45%.

The applied load on the pin shows 83.57% influence on the wear rate, and load was the most influencing parameter which causes the increase in wear rate, followed by disc speed, which shows some influence of 7.07% on wear rate. The B_4C reinforcement shows some negligible impact on the wear rate. The interaction between the parameters shows to be insignificant on the wear values so their effect on the wear rate was not considered. The analysis was carried out with the confidence level of 95% and level of significance of 0.05. The R^2 calculated was 96.50% and was well fitted with in the adjusted limit. Similar observations were made in our previous work [20], where applied load shows significant influence on the wear rate.

4.4 Regression model

Linear regression model was developed from the wear data using Minitab 16 software and it was presented by Eq. (1).

$$\text{Wear rate} = -0.0632 + 0.0188(L) + 0.000272(S) - 0.0126(R), \quad (1)$$

where, L is the load on the pin in N, S is the disc speed in rpm, R is the % of reinforcement.

The confirmation test was carried out using different sets of parameters to match the expected values of the wear and the significance of the developed regression model. Table 7 shows the results of regression model wear value for the same set of parameters and experimental wear value. The error obtained between the predicted wear value using regression model and experimental wear value was within the acceptable limit of 0.05.

4.5 Evaluation of wear mechanism

Figure 10 indicates the SEM images of the worn surfaces for different samples. The wear mechanism of the worn surfaces was influenced by different factors. The

Table 7: Confirmation experiment results

Response	Selected parameters	Regression model value (g/min)	Confirmation experiment value (g/min)	Difference in value
Wear rate	15 N, 200 rpm, 6wt%	0.1772	0.2189	0.04

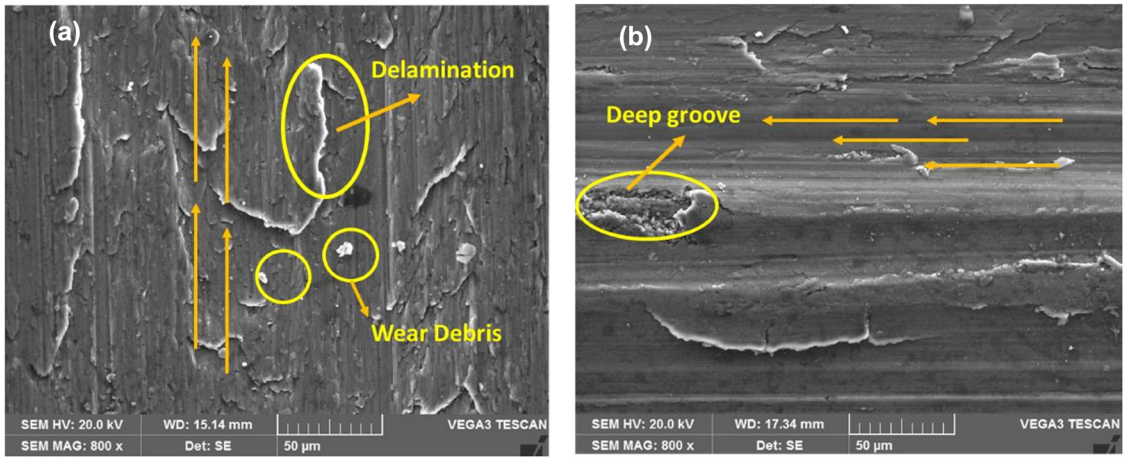

Figure 10: SEM images of the wear samples: (a) 25 N load, 300 rpm speed, and 4 wt% of B_4C and (b) 15 N load, 200 rpm speed, and 2 wt% B_4C.

experimental results showed that the applied load had major contribution on wear. When the load increases, the material removal rate increases and the friction between the pin and the steel disc surface increases.

The effect of disc speed reveals a sensible increase in the wear loss. It indicates that during low load, increase in disc speed shows an increase in loss due to higher interface temperature and molecular smoothening due to heat. The metal wear rate was severe in high load condition, mean after the metal removed from the surface of the pin and the oxide surface was developed when the gap created during metal removal. During that condition, the filler plays an important role in friction behavior of the composite. At low load condition, the oxide layer forms a low coefficient of friction (COF) and makes less the shear strength and less ductility. At high load, high COF leads to protective oxide layer that reduces the chances of further metal removal. Basavarajappa *et al.* [27] revealed that the Gr particles act as a self-lubricating and strain at the interface and reduce the COF. The hard Cu particles present in the composite decreases the high friction force between the pin and disc material. During high load condition, the shear load was carried by this hard Cu particles and reduces further the metal removal rate and reduces the high frictional heat during sliding.

Due to dry sliding between the pin and disc, higher shear forces will generate and cause the soft metal to abrade. That develops the small debris to wear out from the sample and settle on the wear tracks. During low load condition, grooves will be developed on the surface of the pin. The small debris will be formed, and they get trapped between the pin and the disc and form a protective layer. Addition of Gr in the composite acts as a self-lubricating agent and minimizes further the wear rate of the samples. The abrasive wear type of mechanism can be seen in the present investigation.

5 Conclusion

Based on the results obtained, the final conclusions are listed below.

Powder compaction method is one of the effective methods of fabrication of Al-based composites. The hard reinforcement particles can be easily incorporated into the alloy powders using powder compaction method. Results clearly shows that the wear performance of the composites are mainly based on different parameters like applied load and sliding speed. But the reinforcement percentage also shows some influence on the wear performance of the composites. The wear performance of the composites can be improved by incorporating different reinforcement particles and by changing the percentage of reinforcement. From the obtained results, it has been observed that the Gr NPs act as a self-lubrication agent by minimizing the wear. The following final conclusions were made from the current research study.

1. The Al–Cu alloys were successfully reinforced with B_4C hard particles and Gr using powder compaction method.
2. Powder particles were uniformly distributed in Al–Cu alloy powder, which ensures that powder metallurgy is one of the successful fabrication methods to manufacture the composites.
3. The wear analysis results indicate that applied load shows major influence on wear rate as compared to the other two parameters.
4. Applied load has 83.57% impact on the wear rate followed by disc speed of 7.07% and B_4C wt% of 5.85%.

Funding information: The authors state no funding involved.

Author contributions: All authors have accepted responsibility for the entire content of this manuscript and approved its submission.

Conflict of interest: The authors reported no potential conflict of interest.

Data availability statement: The data that are used in findings of this study are available on request basis from the corresponding author. However, the data are available due to privacy/ethical restrictions.

References

[1] Sankar C, Gangatharan K, Christopher Ezhil Singh S, Krishna Sharma R, Mayandi K. Optimization on tribological behaviour of milled nano-B_4C particles reinforced with AZ91 alloy through powder metallurgy method. Trans Indian Inst Met. 2019 May;72(5):1255–75.

[2] Kaushik N, Singhal S. Hybrid combination of Taguchi-GRA-PCA for optimization of wear behavior in AA6063/SiCp matrix composite. Prod Manuf Res. 2018;6(1):171–89.

[3] Ajeel SA, Yaseen RS, Keqal A. The behavior of dry sliding wear for aluminium bronze alloy reinforced by Al_2O_3 and TiO_2 nanoparticles. IOP Conf Ser: Mater Sci Eng. 2019;518(3):032045.

[4] Singh R, Shadab M, Dash A, Rai RN. Characterization of dry sliding wear mechanisms of AA5083/B_4C metal matrix composite. J Braz Soc Mech Sci Eng. 2019 Feb;41(2):1–11.

[5] Manivannan I, Ranganathan S, Gopalakannan S, Suresh S. Mechanical properties and tribological behavior of Al6061–SiC–Gr self-lubricating hybrid nanocomposites. Trans Indian Inst Met. 2018 Aug;71(8):1897–911.
[6] Harichandran R, Selvakumar N, Venkatachalam G. High temperature wear behaviour of nano/micro B_4C reinforced aluminium matrix composites fabricated by an ultrasonic cavitation-assisted solidification process. Trans Indian Inst Met. 2017 Jan;70(1):17–29.
[7] Qiu F, Gao X, Tang J, Gao YY, Shu SL, Han X, et al. Microstructures and tensile properties of Al–Cu matrix composites reinforced with nano-sized SiCp fabricated by semi-solid stirring process. Metals. 2017 Feb 8;7(2):49.
[8] Pan Y, Xiao S, Lu X, Zhou C, Li Y, Liu Z, et al. Fabrication, mechanical properties and electrical conductivity of Al_2O_3 reinforced Cu/CNTs composites. J Alloy Compd. 2019 Apr 25;782:1015–23.
[9] Koga GY, e Silva AM, Wolf W, Kiminami CS, Bolfarini C, Botta WJ. Microstructure and mechanical behavior of $Al_{92}Fe_3Cr_2X_3$ (X= Ce, Mn, Ti, and V) alloys processed by centrifugal force casting. J Mater Res Technol. 2019 Apr 1;8(2):2092–7.
[10] Kim K, Kim D, Park K, Cho M, Cho S, Kwon H. Effect of intermetallic compounds on the thermal and mechanical properties of Al–Cu composite materials fabricated by spark plasma sintering. Materials. 2019 May 10;12(9):1546.
[11] Güler Ö, Bağcı N. A short review on mechanical properties of graphene reinforced metal matrix composites. J Mater Res Technol. 2020 May 1;9(3):6808–33.
[12] Kumar H, Prasad R, Kumar P, Tewari SP, Singh JK. Mechanical and tribological characterization of industrial wastes reinforced aluminum alloy composites fabricated via friction stir processing. J Alloy Compd. 2020 Aug 5;831:154832.
[13] Mei LY, Sun J, Li Y, Lei YY, Du XD, Wu YC. Fabrication of composite modified layer on aluminium alloy by surface mechanical nano-alloying combined with nitriding. Appl Surf Sci. 2020 Jan 1;499:143915.
[14] Bhoi NK, Singh H, Pratap S. Developments in the aluminum metal matrix composites reinforced by micro/nano particles–a review. J Compos Mater. 2020 Mar;54(6):813–33.
[15] Castañeda-Vía J, Landauro CV, Quispe-Marcatoma J, Champi A, Montalvo F, Delgado L, et al. Improvement of mechanical properties of hydroxyapatite composites reinforced with i-$Al_{64}Cu_{23}Fe_{13}$ quasicrystal. J Compos Mater. 2021 Apr;55(9):1209–16.
[16] Weng S, Ning H, Fu T, Hu N, Zhao Y, Huang C, et al. Molecular dynamics study of strengthening mechanism of nanolaminated graphene/Cu composites under compression. Sci Rep. 2018 Feb 15;8(1):1.
[17] Singh SC, Selvakumar N. Effect of milled B_4C nanoparticles on tribological analysis, microstructure and mechanical properties of Cu–4Cr matrix produced by hot extrusion. Arch Civ Mech Eng. 2017 Feb 1;17(2):446–56.
[18] Bongale AM, Kumar S, Sachit TS, Jadhav P. Wear rate optimization of Al/SiCnp/e-glass fibre hybrid metal matrix composites using Taguchi method and genetic algorithm and development of wear model using artificial neural networks. Mater Res Express. 2018 Mar 7;5(3):035005.
[19] Baradeswaran A, Vettivel SC, Perumal AE, Selvakumar N, Issac RF. Experimental investigation on mechanical behaviour, modelling and optimization of wear parameters of B_4C and graphite reinforced aluminium hybrid composites. Mater Des. 2014 Nov 1;63:620–32.
[20] Sachit TS, Mohan N. Wear rate optimization of tungsten carbide (WC) nano particles reinforced aluminum LM4 alloy composites using Taguchi techniques. Mater Res Express. 2019 Mar 27;6(6):066564.
[21] Sachit TS, Mohan N, Suresh R, Prasad MA. Optimization of dry sliding wear behavior of aluminum LM4-Ta/NbC nano composite using Taguchi technique. Mater Today Proc. 2020 Jan 1;27:1977–83.
[22] Ahmad KR, Jamaluddin SB, Hussain LB, Ahmad ZA. The influence of alumina particle size on sintered density and hardness of discontinuous reinforced aluminum metal matrix composite. J Teknologi. 2005;42(A):49–57.
[23] Sharma P, Khanduja D, Sharma S. Tribological and mechanical behavior of particulate aluminum matrix composites. J Reinforced Plast Compos. 2014 Dec;33(23):2192–202.
[24] Manjunatha B, Niranjan HB, Satyanarayana KG. Effect of amount of boron carbide on wear loss of Al-6061 matrix composite by Taguchi technique and rsponse surface analysis. IOP Conf Ser: Mater Sci Eng. 2018;376(1):012071.
[25] Karazi S, Moradi M, Benyounis K. Statistical and numerical approaches for modelling and optimising Laser micromachining process-review. Ref Module Mater Sci Mater Eng. 2019 Apr 29.
[26] Prabhakar NS, Radhika N, Raghu R. Analysis of tribological behavior of aluminium/B_4C composite under dry sliding motion. Procedia Eng. 2014 Jan 1;97:994–1003.
[27] Basavarajappa S, Chandramohan G, Mukund K, Ashwin M, Prabu M. Dry sliding wear behavior of Al 2219/SiCp-Gr hybrid metal matrix composites. J Mater Eng Perform. 2006 Dec;15(6):668–74.